THE JOURNAL OF BIOLOGICAL CHEMISTRY VOL. 291, NO. 3, pp. 1221–1234, January 15, 2016

Lifeguard Inhibits Fas Ligand-mediated Endoplasmic Reticulum-Calcium Release Mandatory for Apoptosis in Type II Apoptotic Cells*

Received for publication, July 8, 2015, and in revised form, November 2, 2015 Published, JBC Papers in Press, November 18, 2015, DOI 10.1074/jbc.M115.677682

Jorge Urresti[‡§], Marisol Ruiz-Meana[¶], Elena Coccia[‡], Juan Carlos Arévalo[‖], José Castellano[¶], Celia Fernández-Sanz[¶], Koen M. O. Galenkamp[‡], Laura Planells-Ferrer[‡§], Rana S. Moubarak[‡], Núria Llecha-Cano[‡], Stéphanie Reix[‡], David García-Dorado[¶1], Bruna Barneda-Zahonero[‡§1,2], and Joan X. Comella[‡§1,3]**

*From the [‡]Cell Signaling and Apoptosis Group and [¶]Laboratory of Experimental Cardiology, Institut de Recerca de l'Hospital Universitari de la Vall d'Hebron, 08035 Barcelona, Spain, the [§]Institut de Neurociències, Departament de Bioquímica i Biologia Molecular, Facultat de Medicina, Universitat Autònoma de Barcelona, 08193 Bellaterra, Spain, the [‖]Department of Cell Biology and Pathology, Instituto de Neurociencias de Castilla y León, Universidad de Salamanca, Salamanca 37007, Spain, and the **Institute of Biomedical Research of Salamanca, Salamanca 37007, Spain*

Death receptors are members of the tumor necrosis factor receptor superfamily involved in the extrinsic apoptotic pathway. Lifeguard (LFG) is a death receptor antagonist mainly expressed in the nervous system that specifically blocks Fas ligand (FasL)-induced apoptosis. To investigate its mechanism of action, we studied its subcellular localization and its interaction with members of the Bcl-2 family proteins. We performed an analysis of LFG subcellular localization in murine cortical neurons and found that LFG localizes mainly to the ER and Golgi. We confirmed these results with subcellular fractionation experiments. Moreover, we show by co-immunoprecipitation experiments that LFG interacts with Bcl-X_L and Bcl-2, but not with Bax or Bak, and this interaction likely occurs in the endoplasmic reticulum. We further investigated the relationship between LFG and Bcl-X_L in the inhibition of apoptosis and found that LFG protects only type II apoptotic cells from FasL-induced death in a Bcl-X_L dependent manner. The observation that LFG itself is not located in mitochondria raises the question as to whether LFG in the ER participates in FasL-induced death. Indeed, we investigated the degree of calcium mobilization after FasL stimulation and found that LFG inhibits calcium release from the ER, a process that correlates with LFG blockage of cytochrome *c* release to the cytosol and caspase activation. On the basis of our observations, we propose that there is a required step in the induction of type II apoptotic cell death that involves calcium mobilization from the ER and that this step is modulated by LFG.

Death receptors (DRs)[4] and their ligands are widely expressed. They can induce either cell survival (1), differentiation (2), or cell death (3). In the latter context, DR stimulation induces the formation of the death-inducing signaling complex (DISC), which leads to caspase activation and nuclear fragmentation.

Fas is a DR expressed in various tissues, including the CNS (4, 5). Cells can be classified by their response to FasL. In type I apoptotic cells, caspase-8 activation is sufficient to induce the activation of executor caspase-3 (6), whereas in type II apoptotic cells, the engagement of these caspases requires a feedback activation loop through the mitochondria (7). Neuronal cells are mainly type II apoptotic cells.

Bcl-2 family members play a key role in regulating cell death (8). The balance between the pro-apoptotic members Bax and Bak and the anti-apoptotic members Bcl-X_L and Bcl-2 controls the permeabilization of the mitochondria. Moreover, Bcl-X_L and Bcl-2 are also localized at the ER (9, 10), where they participate in regulating calcium signals, which are also involved in apoptosis regulation (11, 12).

DR activity can be modulated by a group of proteins called DR antagonists, such as FLIP (13), FAIM-L (Fas apoptotic inhibitory molecule) (14), and LFG. LFG is also known as FAIM2 or transmembrane Bax inhibitory motif (TMBIM) 2 (15). It was discovered in a screening for genes that conferred resistance to Fas-induced apoptosis (16). LFG is highly, although not exclusively, expressed in the nervous system, especially in the hippocampus and the cerebellum (17). Although its location in lipid rafts in the plasma membrane has been reported (18), other studies have described its presence at the Golgi (19). LFG expression is influenced by the PI3K/Akt pathway (20), and the down-regulation of this protein renders cerebellar granule neurons sensitive to Fas-induced apoptosis (21). LFG also has cytoprotective effects in models of ischemia (22). Despite all these findings, the mechanism of action underlying LFG-mediated protection is poorly understood.

* This work was funded by the Spanish Government Ministerio de Sanidad, Servicios Sociales e Igualdad (CIBERNED) Grants CB06/05/1104 (to J. X. C.), PIE13/00027 (to D. G.-D. and J. X. C. and BFU2008-00162 (to J. C. A.); Ministerio de Economía y Competitividad Grants SAF2010-19953 and SAF2013-47989-R (to J. X. C.) and BFU2011-22898 (to J. C. A.), and Generalitat de Catalunya Grants 2011FI_B 00581 (to J. U.) and 2014SGR-1609 (to J. X. C.). The authors declare that they have no conflicts of interest with the contents of this article.

[1] Senior co-authors.

[2] To whom correspondence may be addressed: Cell Signalling and Apoptosis Group, Passeig Vall d'Hebron 119–129, 08035 Barcelona, Spain. Tel.: 34-934893807; Fax: 34-932746708; E-mail: bruna.barneda@vhir.org.

[3] To whom correspondence may be addressed: Cell Signalling and Apoptosis Group, Passeig Vall d'Hebron 119–129, 08035 Barcelona, Spain. Tel.: 34-934893807; Fax: 34-932746708; E-mail: joan.comella@vhir.org.

[4] The abbreviations used are: DR, death receptor; C-ter, C-terminal; DISC, death-inducing signaling complex; ER, endoplasmic reticulum; FasL, Fas ligand; FLIP, FLICE inhibitory protein; LFG, lifeguard; N-ter, N-terminal; TMBIM, transmembrane Bax inhibitory motif; ANOVA, analysis of variance.

Here we performed a study to elucidate the detailed subcellular distribution of LFG. We demonstrate that it localizes mainly at the ER membrane of neurons, whereas no co-localization with mitochondria markers was found. We also studied the relation of LFG with Bcl-2 family members, showing that it interacts with Bcl-X_L and Bcl-2 but not with Bax or Bak. In addition, we also demonstrate that LFG overexpression protects type II apoptotic cells, but not type I, from FasL-induced apoptosis and that this protection depends on the endogenous expression of Bcl-X_L. Additionally, LFG was found to modulate calcium release from the ER after FasL treatment. Our results suggest a novel function of LFG in the ER relevant to Fas-mediated cell death.

Experimental Procedures

Reagents—Recombinant human FasL expressing plasmid was a generous gift from Pascal Schneider (23). Fluorogenic caspase substrate Ac-DEVD-afc was purchased from Calbiochem/Merck Biosciences. Unless otherwise specified, all biochemical reagents were supplied by Sigma-Aldrich.

Plasmids—LFG, LFG-FLAG, 3×HA-Bcl-X_L, Bcl-2, 3×HA-Bax, 3×HA-Bad, and 3×HA-FLIP were expressed under the control of a cytomegalovirus constitutive promoter in the pcDNA3 expression vector (Invitrogen). LFG, Bcl-X_L, and FLIP cDNAs were also subcloned into the pEIGW vector, giving rise to the lentiviral LFG-, Bcl-X_L-, and FLIP-overexpressing plasmids.

For RNAi experiments, constructs were generated in pSUPER.retro.puro (OligoEngine) using specific oligonucleotides targeting Bcl-X_L and LFG sequences as follows: shBcl-X_L, GATTGCAAGTTGGATGGCC; and shLFG, GGAGAGAAGGATGCTC. The control scrambled sequence was GGTCCCTTTCTCTGTAGT. Adaptors to clone the oligonucleotides into the BglII/HindIII sites of pSUPy.retro.puro were added as required. Oligonucleotides were obtained from Sigma-Aldrich. Lentiviral constructs were generated by digesting pSUPER-sh with EcoRI and ClaI to replace the H1 promoter with the H1-shRNA cassette in pLVTHM.

Truncated forms of LFG were amplified from LFG-FLAG-pcDNA3 plasmid using the following primers: Fw-LFG-N-ter, CCCAAGCTTATGACCCAGGGAAAGCTCTCTGTGGCT; Rv-LFG-N-ter, TTGCGGCCGCAAGAGCCGACGAACTTTCTGGTCAT; Fw-LFG-C-ter, CGGAATTCCGTTCATCAGAAAGGTCTATACCATCCT; and Rv-LFG-C-ter, AAAGCGGCCGCTCAGGATCCTTCCCGGTTGGTGC. For the N-ter-LFG construct, amplified cDNA was digested with HindIII/NotI and inserted into the pcDNA3 plasmid. For the C-ter-LFG construct, amplified cDNA was digested with EcoRI/NotI and inserted into the pcDNA3 plasmid.

Lentiviral Production—HEK293T cells were seeded at a density of 2.5×10^6 cells in 0.1% collagen-coated 100-mm dishes. The following day, cells were transfected with 20 μg of pLVTHM-derived constructs, 13 μg of pSPAX2, and 7 μg of pM2G. The transfection was routinely performed by the calcium phosphate transfection method. Cells were allowed to produce lentiviruses for 48 h. After 48 h, the medium was centrifuged at 1200 × *g* for 5 min, and the supernatant was filtered using 45-μm filters. Lentiviruses were concentrated at 50,000 × *g* for 90 min and then resuspended in 20 μl of PBS containing 1% BSA. Lentiviruses were stored at −80 °C. Biological titers of the viral preparations expressed as a number of transducing units/ml were determined by transducing HEK293T cells in limiting dilutions. After 48 h of incubation, the percentage of GFP-positive cells was counted, and viruses at 5×10^8 transducing units/ml were used in the experiments.

Cell Culture—HEK293T, HEK293, and SK-N-AS cells were cultured in DMEM supplemented with 10% heat-inactivated fetal bovine serum (Invitrogen), 20 units/ml penicillin, and 20 μg/ml streptomycin. Cell culture plates were kept at 37 °C in a humidified incubator with 5% CO_2, 95% air.

Female C57BL/6 mice were killed and manipulated following the experimental protocol approved by the Vall d'Hebron Institutional Review Board. Embryonic cerebral cortices were dissected from mouse embryos at day 16. Cells were counted and resuspended in DMEM with glutamine supplemented with 5% heat-inactivated FBS and 5% heat-inactivated fetal horse serum, 20 units/ml penicillin, and 20 μg/ml streptomycin. Cells were seeded in 25 mg/ml poly-L-lysine-coated plates at a density of 1.6×10^5 cells/cm^2. Cell culture plates were kept at 37 °C in a humidified incubator with 5%CO_2/95%air.

Cell Transfection and Infection—HEK293T, HEK293, and SK-N-AS cells were transfected with the desired expression plasmids using Lipofectamine 2000 (Invitrogen), following the manufacturer's instructions.

For lentiviral-based knockdown experiments, SK-N-AS cells were seeded in 60-mm plates at a density of 1×10^5 cells/ml. Titrated lentiviruses were added to the medium when seeding, and medium was changed after 24 h. Transduction efficiency was monitored by direct observation of GFP-positive cells.

Western Blot—Cells were harvested and rinsed once with ice-cold 1× PBS, pH 7.2, and lysed in immunoprecipitation lysis buffer (20 mM Tris, pH 7.4, 140 mM NaCl, 10% glycerol, 2 mM EDTA, 1 mM EGTA, and 1% Triton X-100) supplemented with 1×EDTA-free Complete protease inhibitor mixture (Roche). They were then centrifuged at 16,000 × *g* at 4 °C for 30 min, and the supernatants were collected. Protein concentration was quantified by a modified Lowry assay (DC protein assay; Bio-Rad). The cell lysates obtained were resolved by SDS-PAGE and transferred onto PVDF Immobilon-P membranes (Millipore). After blocking with 1× TBS, 0.1% Tween 20 containing 5% nonfat dry milk for 1 h at room temperature, membranes were probed with the appropriate primary antibodies. They were then incubated for 1 h with the appropriate specific peroxidase-conjugated secondary antibody. Membranes were developed using the EZ-ECL chemiluminescence detection kit (Biological Industries).

The following primary antibodies were used: anti-FLAG (1:20000; Sigma), anti-LFG (1:200; Santa Cruz), anti-HA (1:2000; Sigma), anti-Bcl-2 (1:1000; BD Biosciences), anti-Bcl-X_L (1:1000; Sigma), anti-GluR2 (1:500; Millipore), anti-Rab5 (1:1000; Cell Signaling), anti-calnexin (1:1000; Cell Signaling), anti-histone H3 (1:1000; Cell Signaling), anti-GAPDH (1:500; Santa Cruz), anti-cytochrome *c* (1:1000; BD Biosciences), and anti-caspase-8 (1:1000; Cell Signaling). Naphtol

Blue staining of the PVDF membrane verified equal loading between lanes.

Immunoprecipitation—Samples were lysed in immunoprecipitation lysis buffer as described above, and lysates were quantified by a modified Lowry assay (DC protein assay; Bio-Rad). 1 mg of total protein was adjusted with immunoprecipitation buffer to achieve a concentration of 1 mg/ml. A total of 20 μl of anti-FLAG M2-agarose-coupled antibody was added to each sample and incubated overnight at 4 °C in an orbital shaker. Beads were then washed twice with immunoprecipitation buffer and three more times with 1× TBS. They were then eluted for 30 min at 4 °C with 80 μl of 1× TBS containing 100 ng/ml of 3× FLAG competitor peptide. After a short spin, supernatants were carefully removed, Laemmli buffer was added, and SDS-PAGE was performed.

Endogenous Immunoprecipitation of Bcl-X_L—Cerebellum was dissected from mice adult brain and homogenized in immunoprecipitation lysis buffer, and protein concentration was monitored as described above. 1 mg of protein in 1 ml was subjected to immunoprecipitation. Lysates were precleared by 30 min of incubation with 20 μl of suspended protein G-agarose conjugated and 0.25 μg/μl of control mouse IgG. Afterward, 1 μg of Bcl-X_L antibody (Sigma) or control mouse IgG (Santa Cruz Biotechnology) were added to each sample and incubated 2 h at 4 °C in an orbital shaker. Then 20 μl of agarose-conjugated protein G suspension was added and incubated overnight in an orbital shaker. Beads were then washed five times in immunoprecipitation buffer. Acidic elution in citrate 0.1 M was performed for 5 min and stopped by 1 M Tris-HCl in a 1:3 proportion. After a short spin, supernatants were carefully removed, Laemmli buffer was added, and SDS-PAGE was performed.

Subcellular Fractionation—Subcellular fractionation was performed as previously described (24). Briefly, adult mouse brain was homogenized in buffer containing 10 mM HEPES, pH 7.4, 2 mM EDTA, 0.32 M sucrose, and protease inhibitor mixture (Roche). Cell homogenates were centrifuged sequentially at 600 × *g* for 10 min to remove nuclei and unbroken cells, 3000 × *g* for 10 min to pellet plasma membrane and heavy intracellular membranes, 15,000 × *g* for 15 min to yield the light membranes, and 100,000 × *g* for 1 h to yield the microsomal (pellet) and cytosolic (supernatant) fractions. Nuclei were extracted from the 600 × *g* pellet with centrifugations at 500 × *g* for 15 min. The supernatants were centrifuged twice at each speed, and the pellets were washed twice by resuspension in homogenization buffer and recentrifugation. Pellets were lysed in SET buffer and quantified by a modified Lowry assay. Laemmli buffer was added, and SDS-PAGE was performed

Cytochrome c Release from the Mitochondria—1 × 10^6 SK-N-AS cells were resuspended in a buffer containing 220 mM mannitol, 70 mM sucrose, 50 mM HEPES-KOH, pH 7.2, 10 mM KCl, 5 mM EGTA, 2 mM $MgCl_2$, and 0.025% digitonin and kept on ice for 5 min. Lysed cells were centrifuged (16,000 × *g*; 5 min; 4 °C), and the supernatant was retained as the cytosolic fraction. The release of cytochrome *c* from the mitochondria to the cytosol was assessed by Western blot.

Caspase Activity—After the indicated treatments, cells were rinsed once with PBS and resuspended in lysis buffer containing 20 mM HEPES/NaOH, pH 7.2, 10% sucrose, 150 mM NaCl, 10 mM DTT, 5 mM EDTA, 1% Triton X-100, 0.1% CHAPS, and 1× EDTA-free Complete protease inhibitor mixture (Roche). The lysates were cleared by centrifugation at 16 000 × *g* at 4 °C for 10 min, and supernatants were quantified by the Bradford method (Bio-Rad). Assays were performed in triplicate using 25 μg of protein in the same specific lysis buffer supplemented with 50 μM of the fluorogenic substrate Ac-DEVD-afc. After incubation for 1 h at 37 °C, plates were read in a fluorimeter using a 360-nm (40 nm bandwidth) excitation filter and a 530-nm (25 nm bandwidth) emission filter.

Cell Viability Assays—For apoptotic nuclear morphology, the cells were seeded in 24-well plates and treated as indicated. They were then fixed with 2% paraformaldehyde and stained with 0.05 μg/ml of Hoechst 33258 for 30 min at room temperature in a buffer composed of 2% paraformaldehyde and 1% Triton X-100. Condensed or fragmented nuclei were counted as dead cells, as described previously (25). The determination of cell death by chromatin condensation was performed in blind testing, counting at least 1000 cells for each data point, and was repeated at least three times in independent experiments.

Immunofluorescence—Embryonic day 16 cortical neurons at 1 day *in vitro* were transduced or not with LFG-FLAG-overexpressing lentiviral particles. Seventy-two hours later they were rinsed with PBS at room temperature and fixed in 4% paraformaldehyde/PBS for 30 min at room temperature. Next, they were washed twice with PBS and subsequently permeabilized and blocked with 5% bovine serum albumin and 0.1% Triton X-100 in PBS for 90 min at room temperature. The cells were incubated overnight with the indicated antibodies, rinsed three times with PBS, and incubated with secondary antibodies as indicated for 1 h at room temperature protected from light. Confocal micrographs were obtained using a FluoView1000 spectral confocal microscope.

The following primary antibodies were used: anti-FLAG (1:2000; Sigma), anti-LFG (1:100, Anaspec), anti-calnexin (1:50; Cell Signaling), anti-Rab11 (1:100; Cell Signaling), anti-GM130 (1:25; BD Biosciences), anti-EEA1 (1:200; BD Biosciences), anti-Rab11 (1:50; BD Biosciences), anti-Rab7 (1:250; Sigma), anti-TGN38 (1:200, Affinity Bioreagents), anti-Bcl-X_L (1:250; Sigma), Mitotracker (Life Technologies), and Lysotracker (Life Technologies). Alexa Fluor 488, 568, and 594 were used as secondary antibodies at a dilution of 1:300.

Image Analysis—Co-localization was quantified in 10–15 randomly chosen cells from each sample using ImageJ (JaCoP) software to calculate Manders' co-localization coefficients (M1 and M2) and Pearson's correlation coefficient (R_r) (26). Threshold values were determined using the method described by Costes (27), incorporated in the JaCoP software. Only pixels whose red and green intensity values were both above their respective thresholds were considered to be pixels with co-localized probes. M1 and M2, corresponding to channel 1 (LFG) or channel 2 (other markers), were then calculated as the fractions of total fluorescence in the region of interest that occurred in these "co-local" pixels (with a higher value indicating more co-localization). The M1 values shown represent mean percentages of co-localization.

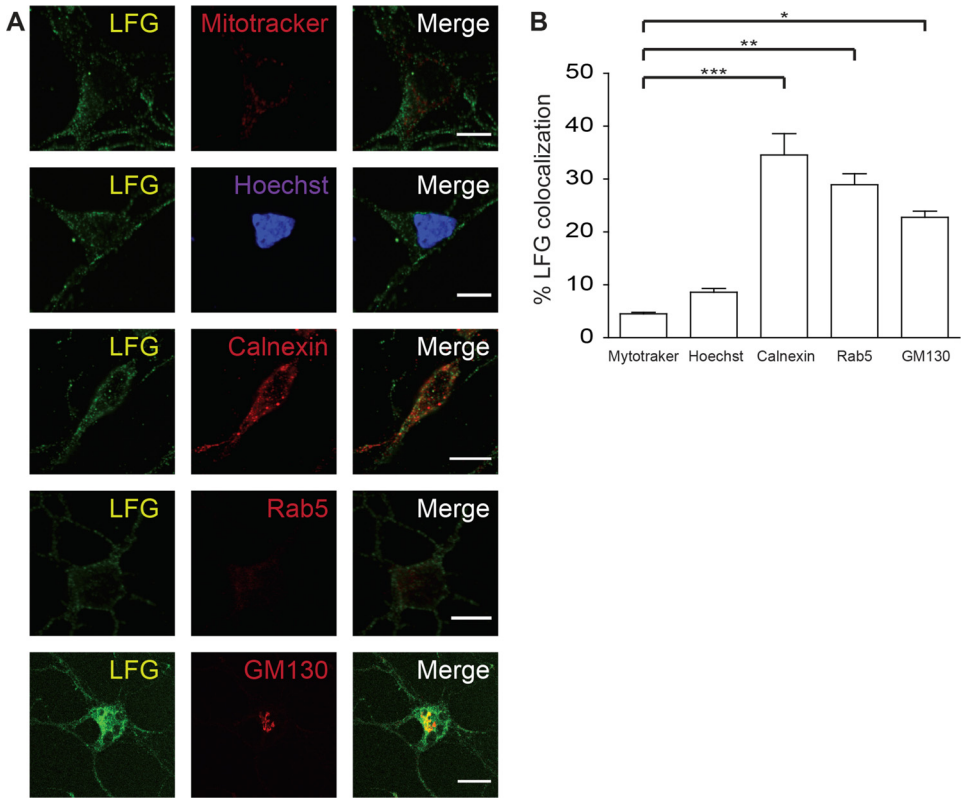

FIGURE 1. **LFG subcellular localization.** *A*, representative confocal images of cortical neurons. Cortical neurons were fixed, permeabilized, and immunostained with anti-LFG (*green*), Mitotracker (mitochondria marker), Hoechst (nucleus marker), anti-calnexin (ER marker), anti-Rab5 (early endosome marker), and anti-GM130 (Golgi marker) (*red*). The *third column* shows a merge of the *green* and *red* channels. *Scale bar*, 10 μm. *B*, Manders' co-localization coefficients for LFG are shown as percentage of LFG co-localization with each marker (one-way ANOVA test). ***, $p \leq 0.001$; **, $p \leq 0.005$; *, $p \leq 0.05$). The values of all Manders' co-localization coefficients and Pearson correlation coefficients for each condition are detailed under "Results."

Cytosolic Calcium Measurements—Cells were incubated in prewarmed control buffer (140 mM NaCl, 3.6 mM KCl, 1.2 mM $MgSO_4$, 1 mM $CaCl_2$, 20 mM HEPES sodium salt, and 5 mM glucose, pH 7.4) in the presence of 5 μM fluo-4 acetoxymethyl ester (F-14201; Molecular Probes) for 30 min at 37 °C, protected from light. Buffer with the dye was washed, and fresh prewarmed control buffer was added.

The cells were excited at 488 nm using an argon/krypton laser confocal system (Yokogawa CSU10, Nipkow spinning disk) set on an Olympus IX70 (VoxCell Scan; Visitech) with a 60× oil immersion objective lens. Emission was captured by a digital CCD camera (ORCA, Hamamatsu, Japan) and analyzed using VoxCell Scan Software (Visitech).

After measurement, each cell in the captured fields was analyzed separately. Cells with a fold-induction of calcium release $\geq$ 1.2 were considered for further analysis. The cells were normalized at the time point they began to react after Fc-FasL treatment.

Statistical Analysis—All the experiments were repeated at least three times. The values are expressed as means ± S.D.

Results

LFG Localizes Mainly at the ER and Golgi Membranes—LFG has been reported to localize at the plasma membrane (18) and *trans*-Golgi network membrane (19); however, a more detailed study of its distribution inside the cell is needed. To determine LFG neuronal subcellular localization, we examined its co-localization with markers of cellular organelles and Manders' co-localization coefficients (M1) and Pearson correlation coefficients (R_r) were obtained for each marker (Fig. 1, *A* and *B*). LFG co-localized with the ER marker calnexin (M1: 34.6 ± 3.6; R_r: 0.562 ± 0.032), the Golgi marker GM130 (M1: 22.8 ± 1.0; R_r: 0.582 ± 0.04), and the early endosome marker Rab5 (M1: 28.9 ± 1.9; R_r: 0.405 ± 0.039). Moreover, LFG presented a finely punctate pattern with some aggregation in the perinuclear region, which suggests an endoplasmic and vesicular localization. In contrast, no significant co-localization was observed with Mitotracker (M1: 4.5 ± 0.3; R_r: 0.105 ± 0.023), a mitochondrial marker, or Hoechst staining (M1: 8.6 ± 2.4; R_r: 0.057 ± 0.038), a nuclear marker (Fig. 1*B*). Thus, these observations suggest that LFG localizes at ER.

LFG Is Localized along the Endocytic Pathway—Because the localization of LFG appears to be vesicular, we sought to study the localization of LFG along the endocytic pathway in greater depth. LFG co-localization with markers of proteins of early, late, and recycling endosomes, lysosomes, as well as markers of the ER and *trans*-Golgi network, was analyzed (Fig. 2*A*). LFG preferentially co-localized with BiP (M1: 77.1 ± 7.7; R_r: 0.715 ± 0.028), an ER marker, as values for coefficients of LFG with these organelles are significantly higher than for endosome markers, EEA1 (M1: 45.8 ± 2.6; R_r: 0.53 ± 0.015), Rab7 (M1: 54.1 ± 2.9; R_r: 0.702 ± 0.032), Rab11 (M1: 56.7 ± 4.8; R_r: 0.666 ± 0.086), Lysotraker (M1: 56.4 ± 3.8; R_r: 0.537 ± 0.031),

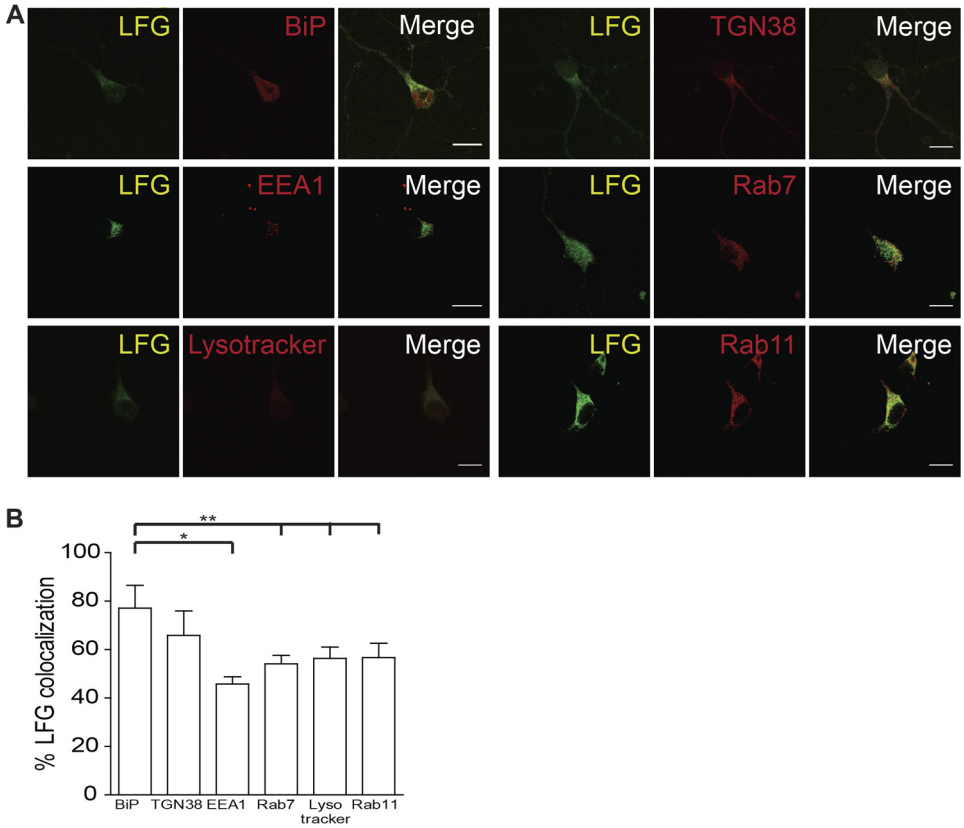

FIGURE 2. **LFG is localized in the endocytic pathway.** *A*, representative confocal images of cortical neurons. Cells were fixed, permeabilized, and immunostained with anti-LFG (*green*) and different elements of the endocytic pathway: anti-BiP (ER marker), anti-TGN38 (*trans*-Golgi network marker), anti-EEA1 (early endosomes marker), anti-Rab7 (late endosome marker), Lysotracker (lysosomal marker), and anti-Rab11 (recycling endosome marker) (*red*). The *third column* shows a merge of the *green* and *red* channels. *Scale bar*, 10 μm. *B*, Manders' co-localization coefficients for LFG are shown as percentages of LFG co-localization with each marker (one-way ANOVA test). **, $p \leq 0.005$; *, $p \leq 0.05$. The values of all Manders' co-localization coefficients and Pearson correlation coefficients for each condition are detailed under "Results."

and TGN38 (M1: 65.9 ± 8.2; R_r: 0.754 ± 0.059) (Fig. 2*B*). Altogether, these results indicate that most cellular LFG in neurons is located at the ER and, to a lesser extent, at the Golgi and vesicular membranes.

LFG Interacts with Bcl-X_L—LFG is a member of the TMBIM family of proteins (28). Some of these members have the capacity to modulate the activity of Bcl-2 family members (29), such as Bcl-X_L and Bcl-2, which are found in mitochondria but also in the ER. We hypothesized that LFG also modulates the activity of Bcl-2 family members in a similar manner. Therefore, we sought to determine LFG interaction with Bcl-2 family proteins. In this regard, we observed that LFG co-immunoprecipitated with Bcl-X_L and Bcl-2 but not with Bax or Bak (Fig. 3*A*).

Because Bcl-X_L and LFG are highly expressed in the CNS (30, 31), we focused our attention on the LFG-Bcl-X_L relationship. To further characterize this interaction, we constructed truncated forms of LFG (Fig. 3*B*). The first 101 amino acids of the LFG sequence, corresponding to the N-ter unfolded domain, were subcloned and fused to a 3×FLAG tag in a pcDNA3 expression vector to form the 3×FLAG-ΔC-LFG construct. The rest of the sequence, corresponding to the transmembrane domain with the C-ter tail, was subcloned along with a FLAG tag and a methionine residue at the start to initiate the open reading frame, forming the ΔN-LFG-FLAG vector. These constructs and LFG-FLAG were overexpressed, along with 3×HA-Bcl-X_L. FLAG immunoprecipitation and HA detection revealed that LFG interacts with Bcl-X_L through its C-ter region (Fig. 3*C*). Endogenous co-localization of LFG with Bcl-X_L in cortical neurons was also studied by immunofluorescence. We observed LFG co-localization with Bcl-X_L (Fig. 3*D*; M1: 47.6 ± 2.9; R_r: 0.558 ± 0.048), located at the cytosol excluding the nucleus, with a stronger staining in the perinuclear region, thereby suggesting ER co-localization. To further confirm the observation that LFG interacts with Bcl-X_L and to rule out possible bias in overexpression experiments, we performed an immunoprecipitation of endogenous Bcl-X_L in lysate from adult mice cerebellum, in which both proteins are highly expressed. We observed that LFG is co-immunoprecipitated with Bcl-X_L (Fig. 3*E*). To study in more detail the localization of LFG-Bcl-X_L interaction, we performed a subfractionation assay in lysate from adult mice brain. LFG is detected in the heavy and light membrane fractions (Fig. 3*F*), further confirming our results about LFG localization in the ER and endocytic vesicles membranes. Moreover, Bcl-X_L is also detected in the heavy and light membranes fraction. Thus, all these data indicate that LFG interacts with Bcl-X_L, and this interaction is likely to occur in the ER membrane.

Although LFG Is Not Localized at the Mitochondria, It Protects Type II Cells from FasL-induced Cell Death—LFG prevents FasL-induced cell death in neurons and neuronal-like cells among others (16, 20), all of them classified as type II apoptotic cells. Nonetheless, there is no direct evidence that LFG protects

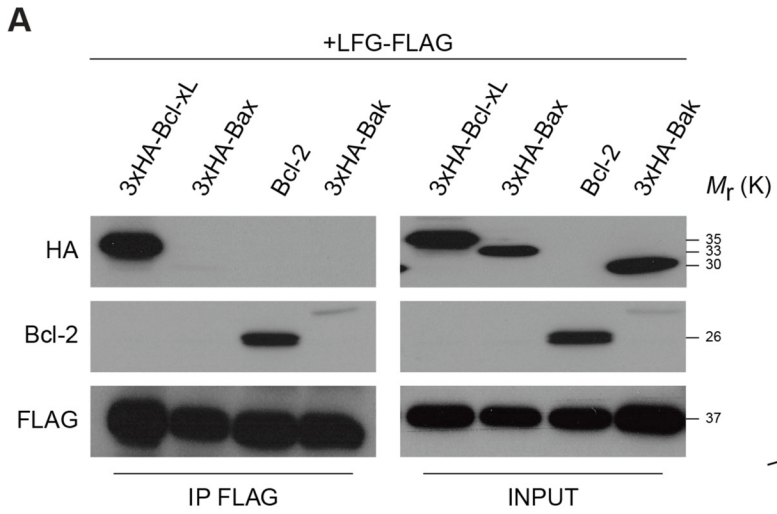
A
+LFG-FLAG
3xHA-Bcl-xL
3xHA-Bax
Bcl-2
3xHA-Bak
3xHA-Bcl-xL
3xHA-Bax
Bcl-2
3xHA-Bak
Mr (K)
HA
Bcl-2
FLAG
35
33
30
26
37
IP FLAG
INPUT

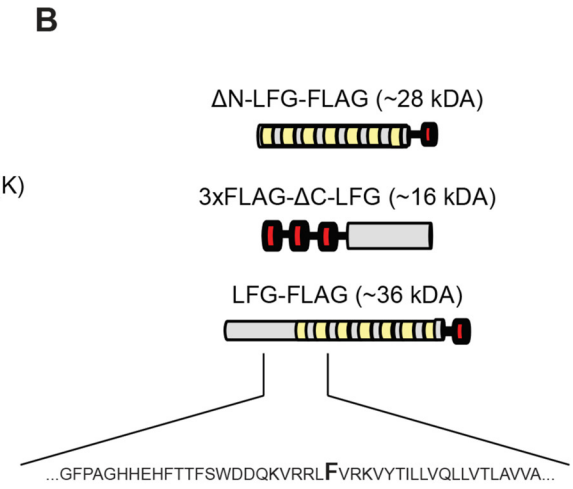
B
ΔN-LFG-FLAG (~28 kDA)
3xFLAG-ΔC-LFG (~16 kDA)
LFG-FLAG (~36 kDA)
...GFPAGHHEHFTTFSWDDQKVRRLFVRKVYTILLVQLLVTLAVVA...

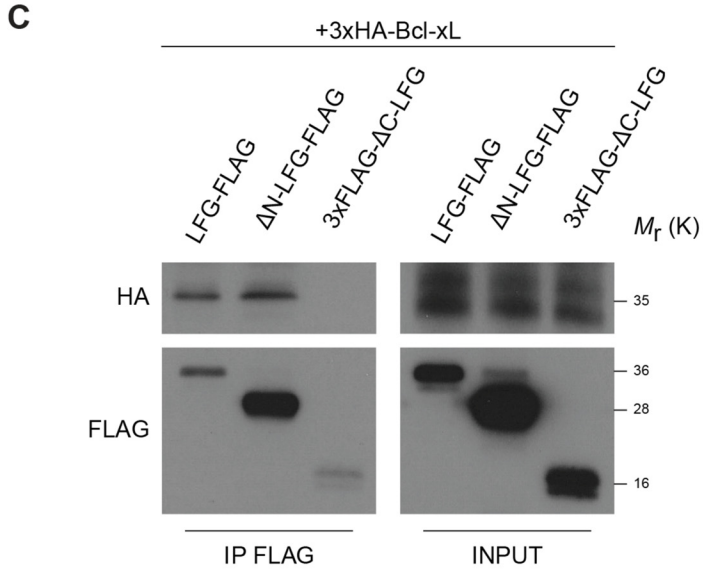
C
+3xHA-Bcl-xL
LFG-FLAG
ΔN-LFG-FLAG
3xFLAG-ΔC-LFG
LFG-FLAG
ΔN-LFG-FLAG
3xFLAG-ΔC-LFG
Mr (K)
HA
FLAG
35
36
28
16
IP FLAG
INPUT

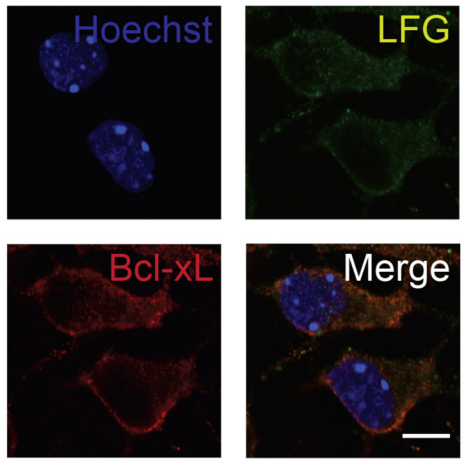
D
Hoechst
LFG
Bcl-xL
Merge

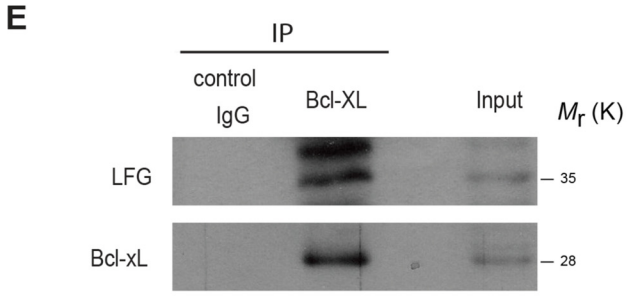
E
IP
control IgG
Bcl-XL
Input
Mr (K)
LFG
Bcl-xL
35
28

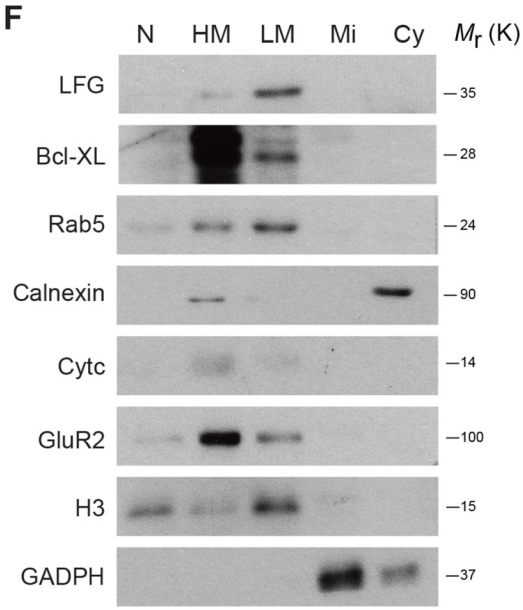
F
N
HM
LM
Mi
Cy
Mr (K)
LFG
Bcl-XL
Rab5
Calnexin
Cytc
GluR2
H3
GADPH
35
28
24
90
14
100
15
37

type I cells against FasL-induced apoptosis. To address this question, we performed a comparative study of LFG inhibition of FasL-induced apoptosis in type I and neuronal-like type II apoptotic cells. To this aim, we overexpressed this protein in parallel with other anti-apoptotic proteins (Bcl-X_L and FLIP) in HEK293 and SK-N-AS cells as models of type I and type II apoptotic cells, respectively. SK-N-AS cells are neuroblastoma-derived cells that are sensitive to Fas-L-induced apoptosis and behave as type II apoptotic cells as expected by their neuronal origin. Bcl-X_L inhibits FasL-induced apoptosis in type II cells but not in type I. FLIP, which competes with caspase-8 for recruitment to the DISC after DR stimulation (32), protects against DR-induced apoptosis in type I and II cells.

Our results show that FasL-induced cell death in SK-N-AS cells, as measured by apoptotic nuclei counting, was inhibited by Bcl-X_L and LFG overexpression at 24 and 48 h after treatment (Fig. 4*C* and data not shown). Such inhibition was not observed in HEK293 cells, where only FLIP overexpression prevented apoptosis (Fig. 4*D*). Moreover, LFG overexpression, as well as that of Bcl-X_L, decreased caspase-3 activation in SK-N-AS (Fig. 4*A*) cells but not in HEK293 cells (Fig. 4*B*). The efficiency of overexpression of the DR antagonists was assessed by Western blot (Fig. 4*G*). Altogether, these data demonstrate that LFG overexpression protects type II apoptotic cells, but not type I apoptotic cells, against Fas-induced cell death.

Requirement of Endogenous Bcl-X_L for LFG Anti-apoptotic Effects—Our findings that LFG protects type II apoptotic cells from Fas-induced cell death and that it interacts with Bcl-X_L suggested that one of these molecules might depend on the other to exert its anti-apoptotic effects. To study this hypothesis, we used SK-N-AS cells, which express both LFG and Bcl-X_L endogenously.

Cells were transduced with lentiviral particles carrying LFG, Bcl-X_L, or Scrambled shRNA, and after 3 days of transduction they were infected again with overexpression lentiviral particles for LFG or Bcl-X_L for 3 additional days. Knockdown efficiency was determined by Western blot (Fig. 5*C*). LFG and Bcl-X_L overexpression reduced caspase 3 activity and the percentage of apoptotic nuclei after Fas-L treatment (Fig. 5, *A* and *B*), in consonance with previous results. However, when Bcl-X_L was down-regulated, LFG overexpression was unable to protect SK-N-AS cells. This was not the case in the opposite situation; thus Bcl-X_L overexpression maintained its anti-apoptotic activity despite endogenous LFG down-regulation (Fig. 5, *A* and *B*). On the basis of these observations, we conclude that endogenous levels of Bcl-X_L are required for LFG anti-apoptotic action, whereas protection from FasL-induced cell death by Bcl-X_L overexpression does not require LFG.

LFG Overexpression Down-regulates Calcium Release from the ER after FasL Stimulation—Calcium transfer from the ER to mitochondria is a crucial step in various forms of cell death (33, 34), including FasL-induced apoptosis, as demonstrated in experiments in Jurkat cells (35). Bcl-X_L exerts anti-apoptotic effects in the ER by blocking calcium release (36, 37). In the same way, BI-1, also known as TMBIM5, modulates calcium release from the ER (29) and has an anti-apoptotic role. Because LFG is also a member of the TMBIM family, and we have demonstrated that it exerts its anti-apoptotic effects in a Bcl-X_L-dependent manner, we hypothesized that it may be involved in the regulation of calcium release from the ER after Fas engagement.

After FasL treatment, SK-N-AS cells released calcium from the ER (Fig. 6*A*), as demonstrated by the lack of calcium release after depletion of the ER calcium content by pretreatment with the sarcoplasmic/endoplasmic reticulum calcium-ATPase inhibitor thapsigargin (Fig. 6*A*). This is the first report involving calcium mobilization from the ER after FasL stimulation in cells from neuronal lineage. In LFG-overexpressing SK-N-AS cells, calcium release from the ER was significantly decreased (Fig. 6, *A* and *D*), and as expected and previously described (36–38), Bcl-X_L overexpression dramatically abrogated calcium release (Fig. 6, *A* and *D*). On the other hand, LFG or Bcl-X_L down-regulation did not significantly alter calcium release from the ER (Fig. 6*B*); nevertheless, these cells showed a tendency to reach higher rates of calcium release than the scrambled control. Strikingly, Bcl-X_L overexpression in shLFG-transduced cells was unable to inhibit calcium release from the ER (Fig. 6*C*). This indicates that Bcl-X_L effects on the ER are dependent on LFG expression, and because these cells are resistant to FasL-induced apoptosis (Fig. 5, *A* and *B*), it suggests that the Bcl-X_L anti-apoptotic effect in the mitochondria is enough to protect from FasL-induced apoptosis. LFG overexpression in shBcl-X_L-transduced cells was unable to prevent calcium release from the ER (Fig. 6*C*), in accordance with previous results that showed a requirement of Bcl-X_L for LFG anti-apoptotic effects. To rule out that the observed effects are not due to changes in ER luminal calcium concentration, we compared the baseline levels of each condition. Baseline levels of intracellular calcium fluorescence were similar in all groups of treatment (data not shown). Our data are in agreement with previously reported studies that point out Bcl-X_L regulation of ER calcium efflux, rather than decreasing intraluminal calcium content, as the mechanism involved in its anti-apoptotic role in the ER (37, 38).

FIGURE 3. **LFG interacts with Bcl-X_L.** *A*, HEK293T cells were transfected with LFG-FLAG expression plasmid and co-transfected with 3×HA-Bcl-X_L, Bcl-2, 3×HA-Bax, or 3×HA-Bad as indicated. FLAG-tagged proteins were immunoprecipitated from whole cell extracts with anti-FLAG resin, followed by immunoblotting HA, Bcl-2, and FLAG antibodies. *B*, schematic representation of LFG-FLAG, ΔN-LFG-FLAG, and 3×FLAG-ΔC-LFG truncated forms. *Green boxes* represent putative transmembrane regions, and *red boxes* the FLAG tag. A fragment of the primary sequence of LFG is shown highlighting the specific amino acid where ΔN-LFG-FLAG ends and 3×FLAG-ΔC-LFG starts. *C*, HEK293T cells were transfected as indicated, and FLAG-tagged proteins were immunoprecipitated from whole cell extracts with anti-FLAG resin, followed by immunoblotting HA and FLAG antibodies. *D*, representative confocal images of cortical neurons. Cortical neurons were fixed, permeabilized, and immunostained with anti-LFG (*green*), anti-Bcl-X_L (*red*), and Hoechst (*purple*). The *lower right panel* shows a merge of all channels. *Scale bar*, 10 μm. The values of all Manders' co-localization coefficients and Pearson correlation coefficients are detailed under "Results." *E*, adult mice cerebellum was homogenized and lysed. Endogenous Bcl-xL was immunoprecipitated, and LFG interaction was assessed by immunoblotting. *F*, adult mice brain was homogenized and lysed. Subfractionation assay was performed, and the different fractions were analyzed by Western blot. LFG and Bcl-xL presence was assessed in each fraction by immunoblotting, and correct purification of each fraction was assessed by immunoblotting with specific markers: anti-Rab5 (early endocytic vesicles), anti-calnexin (ER marker), anti-cytC (mitochondria marker), anti-GluR2 (plasma membrane marker), anti-H3 (nucleus marker), and anti-GADPH (cytosol marker). *N*, nucleus; *HM*, heavy membranes; *LM*, light membranes; *Mi*, microsomal fraction; *Cy*, cytosolic fraction; *IP*, immunoprecipitation.

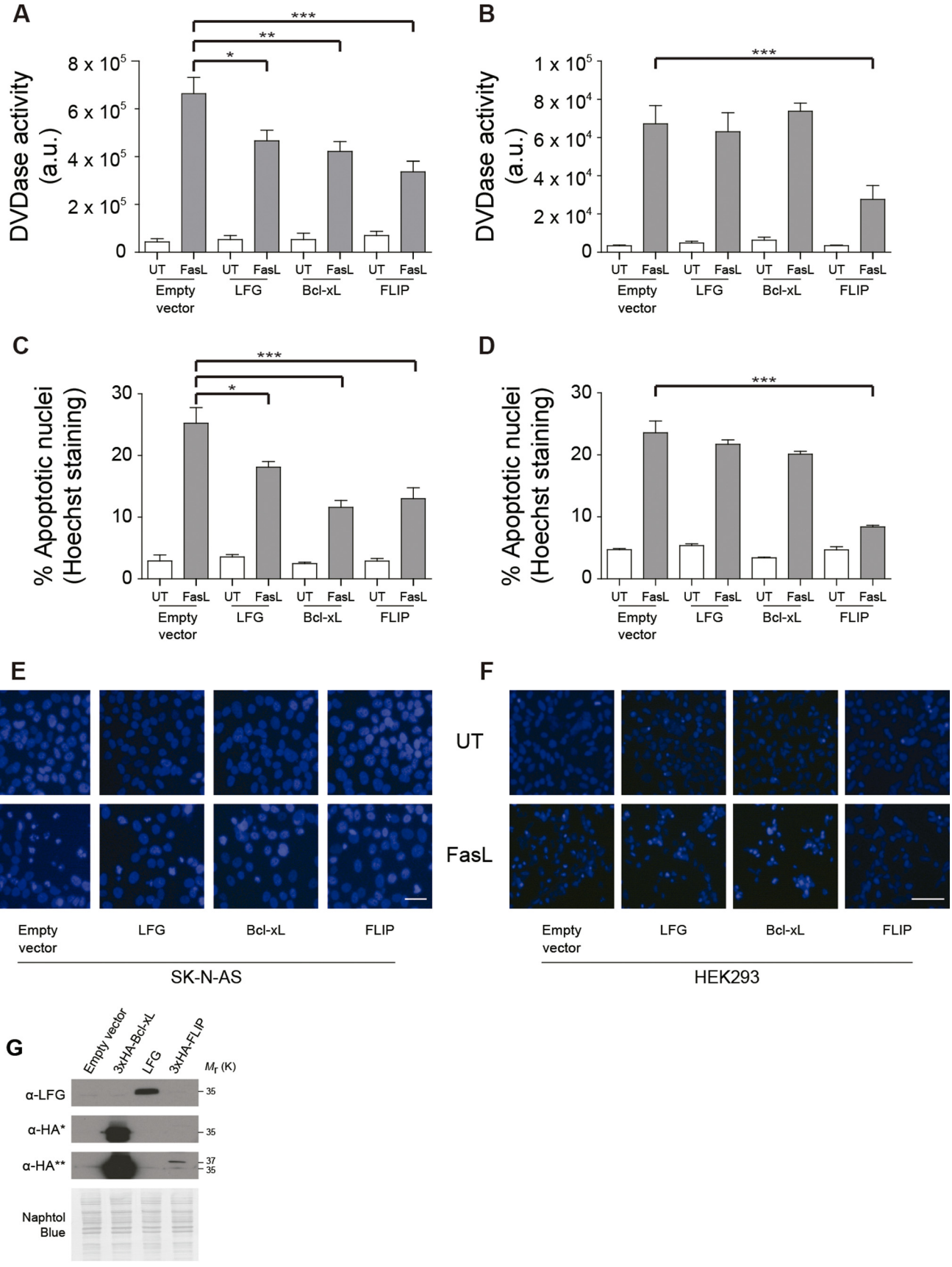
A
DVDase activity (a.u.)
8 x 10^5
6 x 10^5
4 x 10^5
2 x 10^5
0
***
**
*
UT FasL UT FasL UT FasL UT FasL
Empty vector
LFG
Bcl-xL
FLIP
B
DVDase activity (a.u.)
1 x 10^5
8 x 10^4
6 x 10^4
4 x 10^4
2 x 10^4
0
***
UT FasL UT FasL UT FasL UT FasL
Empty vector
LFG
Bcl-xL
FLIP
C
% Apoptotic nuclei (Hoechst staining)
30
20
10
0
***
*
UT FasL UT FasL UT FasL UT FasL
Empty vector
LFG
Bcl-xL
FLIP
D
% Apoptotic nuclei (Hoechst staining)
30
20
10
0
***
UT FasL UT FasL UT FasL UT FasL
Empty vector
LFG
Bcl-xL
FLIP
E
Empty vector
LFG
Bcl-xL
FLIP
SK-N-AS
F
UT
FasL
Empty vector
LFG
Bcl-xL
FLIP
HEK293
G
Empty vector
3xHA-Bcl-xL
LFG
3xHA-FLIP
M_r (K)
α-LFG
35
α-HA*
35
α-HA**
37
35
Naphtol Blue

In summary, LFG and Bcl-X_L overexpressing cells showed a marked reduction in calcium release after FasL treatment when compared with sh scrambled-transduced cells (Fig. 6*A*), whereas down-regulation of LFG or Bcl-X_L did not induce a significant increase (Fig. 6*B*). Overexpression of LFG in shBcl-X_L-transduced cells showed no effect, in the same way as Bcl-X_L overexpression in shLFG-transduced cells (Fig. 6*C*). Taken together, these results suggest that LFG anti-apoptotic effects are mediated by inhibition of calcium release from the ER and that Bcl-X_L is essential for this step. Notably, Bcl-X_L effects on calcium release also appear to be dependent on LFG expression.

FasL-induced Calcium Release from the ER Is Mediated by Caspase-8 Activation in Neuron-like Cells—It has been reported that ER calcium release is mediated by caspase-8 activation and the cleavage of its substrate Bap31 in Jurkat cells after Fas-L stimulation (35, 39). We decided to explore this pathway in our neuronal-like model SK-NA-S cells. Effectively, we observed that ER calcium release after FasL treatment was dependent on caspase-8 activation, because no calcium release from the ER was detected after FasL stimulation when cells were pretreated with the caspase-8 inhibitor IETD (Fig. 7*A*). We also observed the cleavage of procaspase-8 in our conditions after FasL treatment (Fig. 7*B*). More importantly, we were able to detect the cleavage of Bap31 in its p20 fragment, which in turn participates in the cytochrome *c* release from the mitochondria by enhancing calcium signals (40) (Fig. 7*C*). The observed cleavage was caspase-8-mediated, because its inhibition by IETD or the competitive antagonist, FLIP, resulted in no cleavage of Bap31. These data indicate that in neuronal-like cells, caspase-8 activation after FasL stimulation is necessary for ER calcium release.

LFG Overexpression Inhibits Cytochrome c Release from the Mitochondria after FasL Stimulation—Because calcium mobilization from the ER to mitochondria has been described as an important step in the inducement of mitochondria permeabilization (35), we sought to study the effects of LFG in this process. After 6 h of FasL treatment, cytochrome *c* could be detected in the cytosolic fraction of sh scrambled-transduced cells (Fig. 7*D*). As has already been described, Bcl-X_L overexpression inhibited mitochondria permeabilization, as it does FLIP. According to the results for calcium release from the ER, LFG-transduced cells showed a marked reduction of cytochrome *c* release to the cytosol after Fas engagement, suggesting that LFG reduction on ER calcium release may be the mechanism through which LFG performs its anti-apoptotic effect.

On the other hand, down-regulation of Bcl-X_L showed no difference in the amount of cytochrome *c* release compared with sh scrambled control cells (Fig. 7*D*), and LFG overexpression in shBcl-X_L-transduced cells was unable to inhibit mitochondria permeabilization, further confirming the dependence of LFG effects on Bcl-X_L endogenous expression. In shLFG-transduced cells, cytochrome *c* was detected in the cytosol as in sh scrambled-transduced cells, and Bcl-X_L overexpression in these cells blocked cytochrome *c* release, suggesting that Bcl-X_L inhibitory function on mitochondria permeabilization is able to protect from cell death despite the calcium release from the ER. In summary, LFG overexpression reduces cytochrome *c* release from the mitochondria. However, LFG failed to inhibit this processes when Bcl-X_L was down-regulated, highlighting the importance of the association between both proteins on LFG anti-apoptotic function.

Discussion

The protein LFG was discovered during screening for genes that confer resistance to Fas-induced cell death (16). Its predicted structure contains seven hypothetical transmembrane domains and one unfolded region at the N-ter of the protein. However, a functional role of the structural domains of LFG has not yet been described. To date, the mechanism by which LFG protects against Fas-mediated apoptosis is still unknown. It has been proposed that this protein acts upstream of caspase-8 activation because it is able to inhibit the activity of this caspase. The finding that LFG interacts with Fas receptor in the lipid raft has revealed this union as the most plausible mechanism of protection (17). However, no differences in the formation of DISC or in the agonist binding to the receptor have been found when LFG is overexpressed (20).

Studies addressing LFG localization show that it is expressed in postsynaptic sites and dendrites (18). However, a clear punctate pattern not only in dendrites but also in the cell body is detectable when using LFG antibodies for immunofluorescence. We observed that LFG is not localized at the mitochondria. Instead, we demonstrate that LFG localizes mainly in the ER and Golgi apparatus. In agreement with this finding, a study addressing other TMBIM family members reported that LFG also localizes at the membranes of the *trans*-Golgi complex (19, 28).

LFG is highly homologous to BI-1 (15). BI-1 blocks the intrinsic pathway that protects cells from DNA-damaging agents and ER stress inducers (41, 42). It interacts with Bcl-X_L in the ER and regulates calcium signaling (29). Fas-mediated apoptosis shares some features with intrinsic death pathways, such as ER stress (43, 44), and promotes a rise in intracellular calcium (45, 46), which mediates some apoptotic features attributed to FasL-induced cell death (35). The cross-talk between the ER and mitochondria and the calcium efflux between them are

FIGURE 4. **LFG protects type II but not type I cells against FasL-induced cell death.** *A*, SK-N-AS cells were transduced with empty plasmid, LFG-, Bcl-X_L-, or FLIP-overexpressing lentiviral particles for 3 days. Cells were treated with Fc-FasL (100 ng/ml) or left untreated (*UT*) for 6 h. DEVDasa activity was assessed (one-way ANOVA test). ***, $p \leq 0.001$; **, $p \leq 0.005$; *, $p \leq 0.05$. *B*, HEK293 cells were transfected with pcDNA3-, LFG-, 3×HA-Bcl-xL-, and 3×HA-FLIP-overexpressing plasmids for 48 h and treated with Fc-FasL (100 ng/ml) or left untreated for 6 h. DEVDasa activity was assessed (one-way ANOVA test). ***, $p \leq 0.001$. *C*, SK-N-AS cells were transduced as in *A*. The cells were treated with Fc-FasL (100 ng/ml) or left untreated for 24 h. The percentage of apoptosis was assessed by counting cells with apoptotic nuclei (one-way ANOVA test). ***, $p \leq 0.001$; *, $p \leq 0.05$. *D*, HEK293 cells were transfected as in *B*. The cells were treated with Fc-FasL (100 ng/ml) or left untreated for 10 h. Percentage of apoptosis was assessed by counting cells with apoptotic nuclei (one-way ANOVA test). ***, $p \leq 0.001$. *E*, representative images of SK-N-AS cells with Hoechst staining, transduced as in *A*, and treated with Fc-FasL (100 ng/ml) or left untreated for 24 h. *Scale bar*, 10 μm. *F*, representative images of HEK293 cells with Hoechst staining, transfected as *B*, and treated with Fc-FasL (100 ng/ml) or left untreated for 24 h. *Scale bar*, 10 μm. *G*, immunoblot analysis was performed to assess LFG, Bcl-X_L and FLIP overexpression in HEK293 cells. *, short exposure; **, long exposure. Naphtol Blue staining was performed to confirm equal loading.

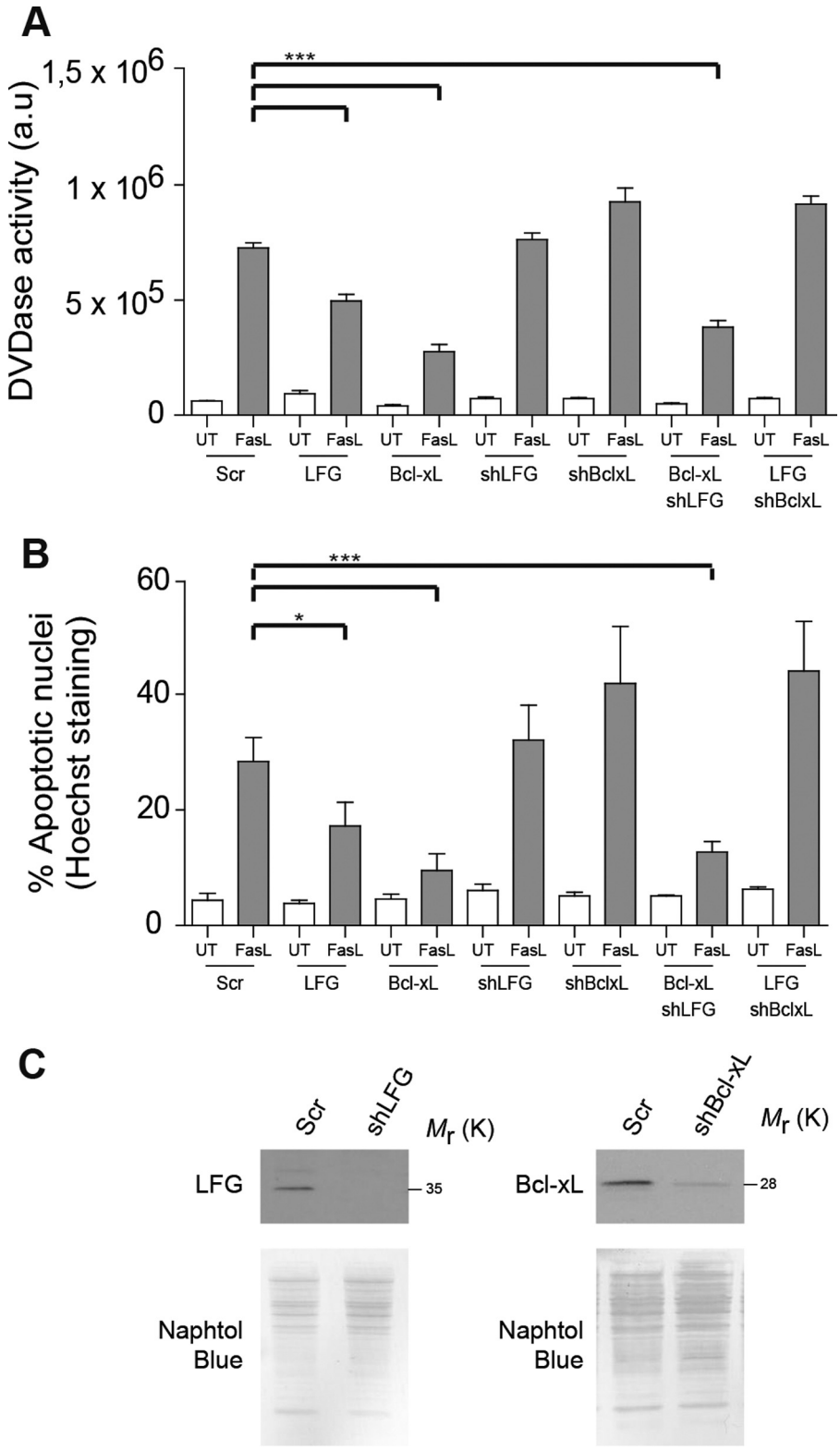

FIGURE 5. **Endogenous Bcl-X_L is essential for LFG protection against FasL-induced cell death.** *A*, SK-N-AS cells were transduced with lentiviral particles carrying shRNA against LFG, Bcl-X_L, or scrambled (*Scr*) for 3 days and then transduced with LFG- or Bcl-X_L-overexpressing lentiviral particles for 3 additional days as indicated. The cells were treated with Fc-FasL (100 ng/ml) or left untreated (*UT*) for 6 h. DEVDasa activity was assessed (one-way ANOVA test). ***, $p \leq 0.001$. *B*, SK-N-AS cells were transduced as in *A*. The cells were treated with Fc-FasL (100 ng/ml) or left untreated for 24 h. The percentage of apoptosis was assessed by counting cells with apoptotic nuclei (one-way ANOVA test). ***, $p \leq 0.001$; *, $p \leq 0.05$. *C*, immunoblot analysis was performed to assess LFG and Bcl-X_L down-regulation in SK-N-AS cells. Naphtol Blue staining was performed to confirm equal loading.

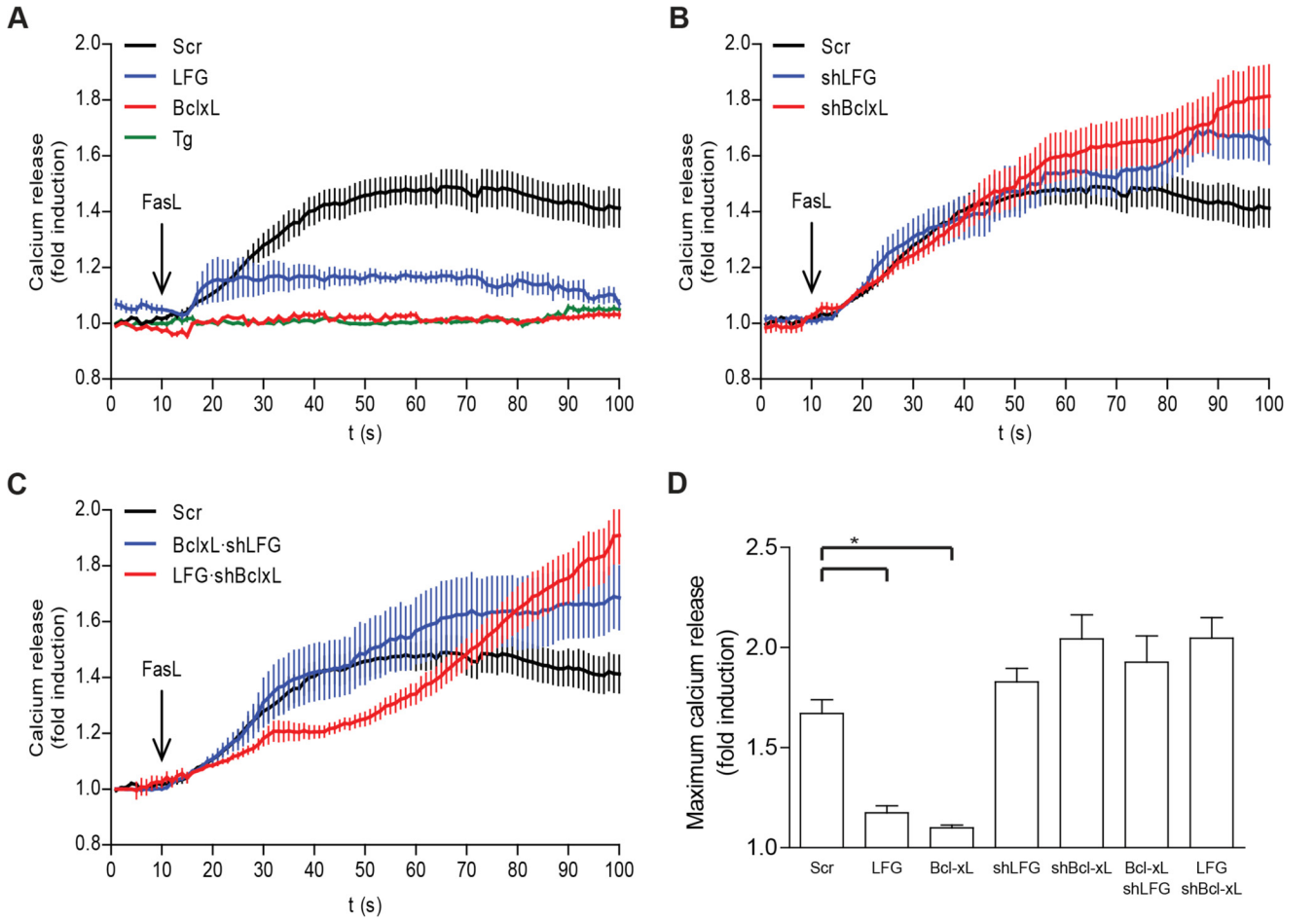

FIGURE 6. **LFG inhibits calcium release from the ER after Fas stimulation.** *A*, SK-N-AS cells were transduced with empty plasmid and LFG- and Bcl-X_L-overexpressing lentiviral particles for 3 days or treated with thapsigargin (*Tg*; 1 μM) for 30 min prior to Fc-FasL (200 ng/ml) treatment. Intracellular calcium mobilization was assessed as detailed under "Experimental Procedures." *B*, SK-N-AS cells were transduced with lentiviral particles carrying shRNA against LFG, Bcl-X_L, or scrambled (*Scr*) for 3 days. Cells were treated with Fc-FasL (200 ng/ml), and intracellular calcium mobilization was assessed. *C*, SK-N-AS cells were transduced with lentiviral particles carrying shRNA against LFG, Bcl-X_L, or scrambled for 3 days and then transduced with LFG- or Bcl-X_L-overexpressing lentiviral particles for 3 additional days as indicated. The cells were treated with Fc-FasL (200 ng/ml), and intracellular calcium mobilization was assessed. *D*, maximum calcium release of SK-N-AS transduced cells, calculated as the average of maximum calcium release of at least 10 individual cells per group (one-way ANOVA test). *, $p \leq 0.05$.

important steps in Fas apoptotic signaling, at least in the immune system (47). Nonetheless, nothing is known in other systems. Thus, we propose that LFG exerts its anti-apoptotic effects by modulating mitochondria permeabilization via an ER-dependent mechanism in the nervous system. LFG inhibits calcium release from the ER after FasL treatment. Accordingly, a marked reduction in cytochrome *c* release, and caspase-8 activation is observed in LFG-transduced cells. However, we observed that LFG effects are Bcl-X_L-dependent. Bcl-X_L overexpression also inhibits calcium release from the ER, and cytochrome *c* release. When LFG is down-regulated, Bcl-X_L is still able to inhibit mitochondria permeabilization and caspases activation; nevertheless, calcium release from the ER remains unaffected.

On the basis of these observations, we suggest that LFG may play a role in the regulation of calcium release from the ER after an apoptotic stimulus. Blockade of the calcium efflux from ER to the mitochondria would be a limiting step to inhibit the cytochrome *c* release and subsequent activation of caspase-3, thereby preventing apoptosis (Fig. 8).

Taking into the account that LFG did not influence ligand binding to Fas-receptor or DISC formation (16), it was suggested that LFG might act at the level of caspase-8 activation. Nevertheless, we report data that contradicts this view. First, we report that LFG is only able to protect type II apoptotic cells, whereas it fails to inhibit apoptosis in type I apoptotic cells. If LFG was able to inhibit caspase-8 activation directly, it should be able to inhibit type-I Fas-induced apoptosis, in the same way as other caspase-8 inhibitors, such as FLIP. In addition, LFG lose its protective effects when Bcl-X_L is down-regulated. Because our data suggest that the interaction between both proteins is essential for LFG function, is highly unlikely that LFG may exert its main effect at the receptor level, where Bcl-X_L is not localized. If LFG effects were located at the DISC level, effects on blockade of calcium release from the ER and prevention of cytochrome *c* release from mitochondria should be observed despite Bcl-X_L down-regulation.

Bcl-X_L plays a central role in the regulation of FasL-induced apoptosis in type II cells. It is located at both the mitochondria and the ER (48, 49), and its anti-apoptotic function through

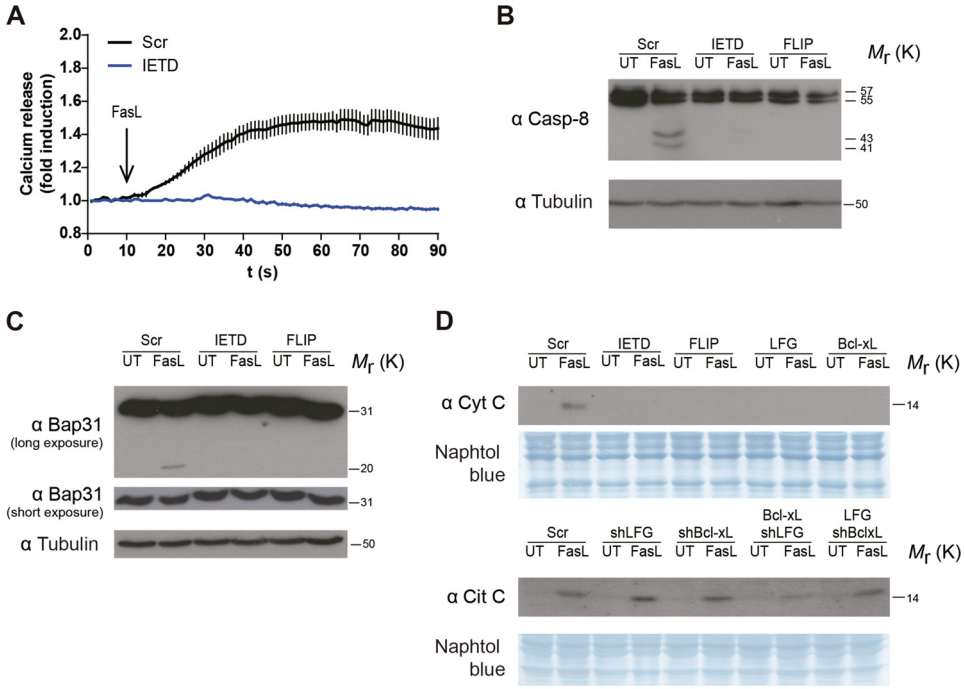

FIGURE 7. **LFG overexpression inhibits cytochrome *c* release from the mitochondria after Fas stimulation.** *A*, SK-N-AS cells were treated with IETD (20 μM) for 30 min prior to Fc-FasL (200 ng/ml) treatment. Intracellular calcium mobilization was assessed. *B* and *C*, SK-N-AS cells were transduced FLIP-overexpressing lentiviral particles for 3 days or treated with IETD (20 μM) as indicated. The cells were treated with Fc-FasL (100 ng/ml) or left untreated (*UT*) for 6 h, and then Western blot was used to assess the cleavage of procaspase-8 (*B*) or Bap31 (*C*). Tubulin was used as loading control. *D*, SK-N-AS cells were transduced with lentiviral particles carrying shRNA against LFG, Bcl-X_L, or scrambled (*Scr*) for 3 days and then transduced with LFG- or Bcl-X_L-overexpressing lentiviral particles for 3 additional days as indicated. Cells were treated with Fc-FasL (100 ng/ml) or left untreated for 4 h. Cytochrome *c* (*Cyt C*) release to the cytosol was assessed by Western blot. Naphtol Blue staining was used as a loading control.

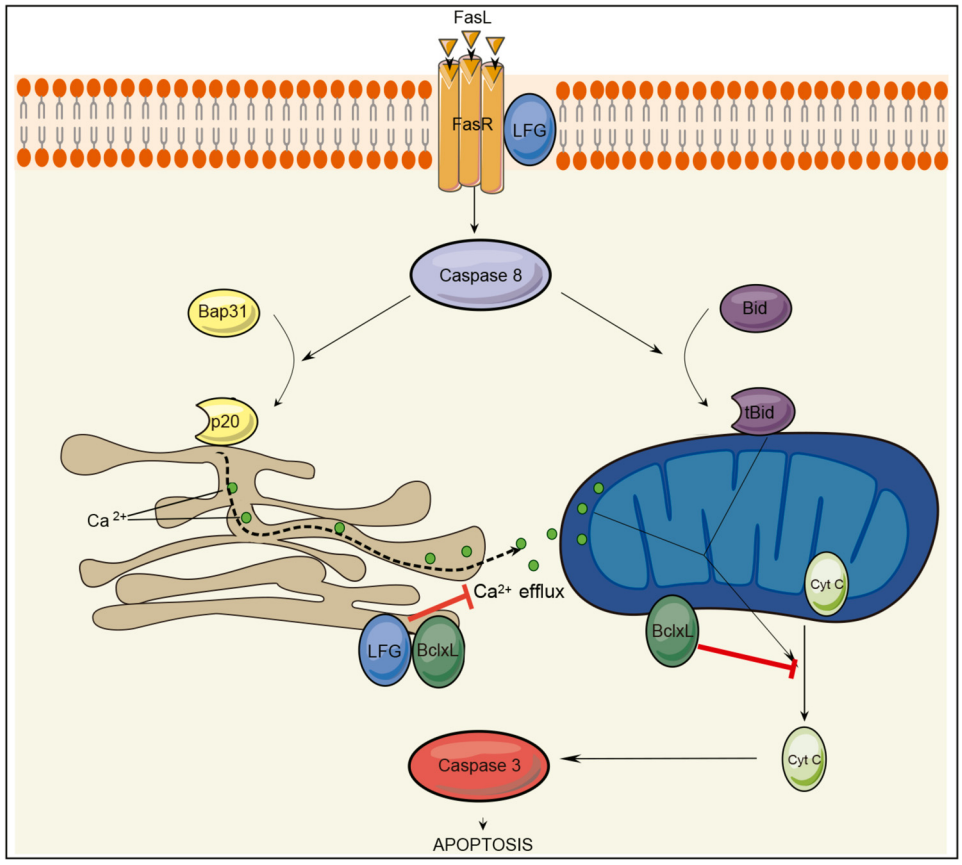

FIGURE 8. **Schematic representation of Fas apoptotic signaling pathway and the hypothetic steps inhibited by LFG.** After Fas stimulation, caspase-8 cleaves Bap31 and tBid. p20 fragment induces Ca^{2+} efflux from the ER to the mitochondria, which in conjunction with tBid induces mitochondrial permeabilization and cytochrome *c* release. Although Bcl-X_L is able to inhibit ER calcium release and mitochondria permeabilization directly, LFG is only able to block the ER step.

both organelles is well documented. Strikingly, Bcl-X_L effects on ER calcium signaling appear to be dependent on LFG endogenous expression.

In summary, our results reveal a hitherto undescribed step in the extrinsic apoptotic signaling pathway in cells from neuronal lineage. Calcium mobilization from the ER has been shown to be relevant in FasL apoptotic signaling. We demonstrate that LFG modulates calcium release from the ER after FasL stimulation and inhibits FasL-induced apoptosis in neuron-like cells that are type II apoptotic cells regarding the way they subside apoptosis. On the basis of our observations, we propose that LFG protects against FasL-induced apoptosis by modulating calcium release from the ER.

Author Contributions—J. X. C., B. B.-Z., S. R., and J. U. designed the project. D. G.-D., J. U., M. R. M., J. C., and C. F.-S. co-designed and performed laboratory work and analyzed the results of calcium release. J. U., J. C. A., E. C. performed and analyzed experiments of LFG localization. J. U., E. C., K. M. O. G., L. P.-F., R. S. M., N. L.-C., and S. R. performed laboratory work and collected the data. J. X. C., B. B.-Z., and J. U., wrote the manuscript. The final manuscript was read and approved by all signing authors.

Acknowledgments—We thank Dr. Didier Trono for providing the lentiviral plasmids, Dr. Pascal Schneider for providing the plasmid encoding recombinant FasL, Marta Valeri for technical help on confocal microscopy, Tanya Yates for helping with the correction of the paper, and Tamara Carretero for technical help on image treatment.

References

1. Marques-Fernandez, F., Planells-Ferrer, L., Gozzelino, R., Galenkamp, K. M., Reix, S., Llecha-Cano, N., Lopez-Soriano, J., Yuste, V. J., Moubarak, R. S., and Comella, J. X. (2013) TNFα induces survival through the FLIP-L-dependent activation of the MAPK/ERK pathway. *Cell Death Dis.* **4,** e493
2. Pasqualetto, V., Vasseur, F., Zavala, F., Schneider, E., and Ezine, S. (2005) Fas receptor signaling is requisite for B cell differentiation. *J. Leukocyte Biol.* **78,** 1106–1117
3. Kaufmann, T., Strasser, A., and Jost, P. J. (2012) Fas death receptor signalling: roles of Bid and XIAP. *Cell Death Differ.* **19,** 42–50
4. Choi, C., and Benveniste, E. N. (2004) Fas ligand/Fas system in the brain: regulator of immune and apoptotic responses. *Brain Res. Brain Res. Rev.* **44,** 65–81
5. Park, C., Sakamaki, K., Tachibana, O., Yamashima, T., Yamashita, J., and Yonehara, S. (1998) Expression of fas antigen in the normal mouse brain. *Biochem. Biophys. Res. Commun.* **252,** 623–628
6. Scaffidi, C., Fulda, S., Srinivasan, A., Friesen, C., Li, F., Tomaselli, K. J., Debatin, K. M., Krammer, P. H., and Peter, M. E. (1998) Two CD95 (APO-1/Fas) signaling pathways. *EMBO J.* **17,** 1675–1687
7. Scaffidi, C., Schmitz, I., Zha, J., Korsmeyer, S. J., Krammer, P. H., and Peter, M. E. (1999) Differential modulation of apoptosis sensitivity in CD95 type I and type II cells. *J. Biol. Chem.* **274,** 22532–22538
8. Youle, R. J., and Strasser, A. (2008) The BCL-2 protein family: opposing activities that mediate cell death. *Nat. Rev. Mol. Cell Biol.* **9,** 47–59
9. Szegezdi, E., Macdonald, D. C., Ní Chonghaile, T., Gupta, S., and Samali, A. (2009) Bcl-2 family on guard at the ER. *Am. J. Physiol. Cell Physiol.* **296,** C941–C953
10. Thomenius, M. J., and Distelhorst, C. W. (2003) Bcl-2 on the endoplasmic reticulum: protecting the mitochondria from a distance. *J. Cell Sci.* **116,** 4493–4499
11. Bonneau, B., Prudent, J., Popgeorgiev, N., and Gillet, G. (2013) Non-apoptotic roles of Bcl-2 family: the calcium connection. *Biochim. Biophys. Acta* **1833,** 1755–1765
12. Distelhorst, C. W., and Shore, G. C. (2004) Bcl-2 and calcium: controversy beneath the surface. *Oncogene* **23,** 2875–2880
13. Irmler, M., Thome, M., Hahne, M., Schneider, P., Hofmann, K., Steiner, V., Bodmer, J. L., Schröter, M., Burns, K., Mattmann, C., Rimoldi, D., French, L. E., and Tschopp, J. (1997) Inhibition of death receptor signals by cellular FLIP. *Nature* **388,** 190–195
14. Schneider, T. J., Fischer, G. M., Donohoe, T. J., Colarusso, T. P., and Rothstein, T. L. (1999) A novel gene coding for a Fas apoptosis inhibitory molecule (FAIM) isolated from inducibly Fas-resistant B lymphocytes. *J. Exp. Med.* **189,** 949–956
15. Hu, L., Smith, T. F., and Goldberger, G. (2009) LFG: a candidate apoptosis regulatory gene family. *Apoptosis* **14,** 1255–1265
16. Somia, N. V., Schmitt, M. J., Vetter, D. E., Van Antwerp, D., Heinemann, S. F., and Verma, I. M. (1999) LFG: an anti-apoptotic gene that provides protection from Fas-mediated cell death. *Proc. Natl. Acad. Sci. U.S.A.* **96,** 12667–12672
17. Fernández, M., Segura, M. F., Solé, C., Colino, A., Comella, J. X., and Ceña, V. (2007) Lifeguard/neuronal membrane protein 35 regulates Fas ligand-mediated apoptosis in neurons via microdomain recruitment. *J. Neurochem.* **103,** 190–203
18. Schweitzer, B., Suter, U., and Taylor, V. (2002) Neural membrane protein 35/Lifeguard is localized at postsynaptic sites and in dendrites. *Brain Res. Mol. Brain Res.* **107,** 47–56
19. Yamaji, T., Nishikawa, K., and Hanada, K. (2010) Transmembrane BAX inhibitor motif containing (TMBIM) family proteins perturbs a *trans*-Golgi network enzyme, Gb3 synthase, and reduces Gb3 biosynthesis. *J. Biol. Chem.* **285,** 35505–35518
20. Beier, C. P., Wischhusen, J., Gleichmann, M., Gerhardt, E., Pekanovic, A., Krueger, A., Taylor, V., Suter, U., Krammer, P. H., Endres, M., Weller, M., and Schulz, J. B. (2005) FasL (CD95L/APO-1L) resistance of neurons mediated by phosphatidylinositol 3-kinase-Akt/protein kinase B-dependent expression of lifeguard/neuronal membrane protein 35. *J. Neurosci.* **25,** 6765–6774
21. Hurtado de Mendoza, T., Perez-Garcia, C. G., Kroll, T. T., Hoong, N. H., O'Leary, D. D., and Verma, I. M. (2011) Antiapoptotic protein Lifeguard is required for survival and maintenance of Purkinje and granular cells. *Proc. Natl. Acad. Sci. U.S.A.* **108,** 17189–17194
22. Reich, A., Spering, C., Gertz, K., Harms, C., Gerhardt, E., Kronenberg, G., Nave, K. A., Schwab, M., Tauber, S. C., Drinkut, A., Harms, K., Beier, C. P., Voigt, A., Göbbels, S., Endres, M., and Schulz, J. B. (2011) Fas/CD95 regulatory protein Faim2 is neuroprotective after transient brain ischemia. *J. Neurosci.* **31,** 225–233
23. Holler, N., Tardivel, A., Kovacsovics-Bankowski, M., Hertig, S., Gaide, O., Martinon, F., Tinel, A., Deperthes, D., Calderara, S., Schulthess, T., Engel, J., Schneider, P., and Tschopp, J. (2003) Two adjacent trimeric Fas ligands are required for Fas signaling and formation of a death-inducing signaling complex. *Mol. Cell. Biol.* **23,** 1428–1440
24. Jacobs, S. B., Basak, S., Murray, J. I., Pathak, N., and Attardi, L. D. (2007) Siva is an apoptosis-selective p53 target gene important for neuronal cell death. *Cell Death Differ* **14,** 1374–1385
25. Yuste, V. J., Bayascas, J. R., Llecha, N., Sánchez-López, I., Boix, J., and Comella, J. X. (2001) The absence of oligonucleosomal DNA fragmentation during apoptosis of IMR-5 neuroblastoma cells: disappearance of the caspase-activated DNase. *J. Biol. Chem.* **276,** 22323–22331
26. McDonald, J. H., and Dunn, K. W. (2013) Statistical tests for measures of colocalization in biological microscopy. *J. Microsc.* **252,** 295–302
27. Costes, S. V., Daelemans, D., Cho, E. H., Dobbin, Z., Pavlakis, G., and Lockett, S. (2004) Automatic and quantitative measurement of protein-protein colocalization in live cells. *Biophys. J.* **86,** 3993–4003
28. Lisak, D. A., Schacht, T., Enders, V., Habicht, J., Kiviluoto, S., Schneider, J., Henke, N., Bultynck, G., and Methner, A. (2015) The transmembrane Bax inhibitor motif (TMBIM) containing protein family: Tissue expression, intracellular localization and effects on the ER CA-filling state. *Biochim. Biophys. Acta* **1853,** 2104–2114
29. Hunsberger, J. G., Machado-Vieira, R., Austin, D. R., Zarate, C., Chuang, D. M., Chen, G., Reed, J. C., and Manji, H. K. (2011) Bax inhibitor 1, a modulator of calcium homeostasis, confers affective resilience. *Brain Res.* **1403,** 19–27

30. Krajewska, M., Mai, J. K., Zapata, J. M., Ashwell, K. W., Schendel, S. L., Reed, J. C., and Krajewski, S. (2002) Dynamics of expression of apoptosis-regulatory proteins Bid, Bcl-2, Bcl-X, Bax and Bak during development of murine nervous system. *Cell Death Differ.* **9,** 145–157
31. Schweitzer, B., Taylor, V., Welcher, A. A., McClelland, M., and Suter, U. (1998) Neural membrane protein 35 (NMP35): a novel member of a gene family which is highly expressed in the adult nervous system. *Mol. Cell. Neurosci.* **11,** 260–273
32. Scaffidi, C., Schmitz, I., Krammer, P. H., and Peter, M. E. (1999) The role of c-FLIP in modulation of CD95-induced apoptosis. *J. Biol. Chem.* **274,** 1541–1548
33. Kobayashi, T., Kuroda, S., Tada, M., Houkin, K., Iwasaki, Y., and Abe, H. (2003) Calcium-induced mitochondrial swelling and cytochrome *c* release in the brain: its biochemical characteristics and implication in ischemic neuronal injury. *Brain Res.* **960,** 62–70
34. Mattson, M. P., and Chan, S. L. (2003) Calcium orchestrates apoptosis. *Nat. Cell Biol.* **5,** 1041–1043
35. Wozniak, A. L., Wang, X., Stieren, E. S., Scarbrough, S. G., Elferink, C. J., and Boehning, D. (2006) Requirement of biphasic calcium release from the endoplasmic reticulum for Fas-mediated apoptosis. *J. Cell Biol.* **175,** 709–714
36. White, C., Li, C., Yang, J., Petrenko, N. B., Madesh, M., Thompson, C. B., and Foskett, J. K. (2005) The endoplasmic reticulum gateway to apoptosis by Bcl-X(L) modulation of the InsP3R. *Nat. Cell Biol.* **7,** 1021–1028
37. Li, C., Wang, X., Vais, H., Thompson, C. B., Foskett, J. K., and White, C. (2007) Apoptosis regulation by Bcl-x(L) modulation of mammalian inositol 1,4,5-trisphosphate receptor channel isoform gating. *Proc. Natl. Acad. Sci. U.S.A.* **104,** 12565–12570
38. Sung, P. J., Tsai, F. D., Vais, H., Court, H., Yang, J., Fehrenbacher, N., Foskett, J. K., and Philips, M. R. (2013) Phosphorylated K-Ras limits cell survival by blocking Bcl-xL sensitization of inositol trisphosphate receptors. *Proc. Natl. Acad. Sci. U.S.A.* **110,** 20593–20598
39. Nguyen, M., Breckenridge, D. G., Ducret, A., and Shore, G. C. (2000) Caspase-resistant BAP31 inhibits fas-mediated apoptotic membrane fragmentation and release of cytochrome *c* from mitochondria. *Mol. Cell Biol.* **20,** 6731–6740
40. Breckenridge, D. G., Stojanovic, M., Marcellus, R. C., and Shore, G. C. (2003) Caspase cleavage product of BAP31 induces mitochondrial fission through endoplasmic reticulum calcium signals, enhancing cytochrome *c* release to the cytosol. *J. Cell Biol.* **160,** 1115–1127
41. Kim, J. H., Lee, E. R., Jeon, K., Choi, H. Y., Lim, H., Kim, S. J., Chae, H. J., Park, S. H., Kim, S., Seo, Y. R., Kim, J. H., and Cho, S. G. (2012) Role of BI-1 (TEGT)-mediated ERK1/2 activation in mitochondria-mediated apoptosis and splenomegaly in BI-1 transgenic mice. *Biochim. Biophys. Acta* **1823,** 876–888
42. Xu, Q., and Reed, J. C. (1998) Bax inhibitor-1, a mammalian apoptosis suppressor identified by functional screening in yeast. *Mol. Cell* **1,** 337–346
43. Bernard-Marissal, N., Moumen, A., Sunyach, C., Pellegrino, C., Dudley, K., Henderson, C. E., Raoul, C., and Pettmann, B. (2012) Reduced calreticulin levels link endoplasmic reticulum stress and Fas-triggered cell death in motoneurons vulnerable to ALS. *J. Neurosci.* **32,** 4901–4912
44. Timmins, J. M., Ozcan, L., Seimon, T. A., Li, G., Malagelada, C., Backs, J., Backs, T., Bassel-Duby, R., Olson, E. N., Anderson, M. E., and Tabas, I. (2009) Calcium/calmodulin-dependent protein kinase II links ER stress with Fas and mitochondrial apoptosis pathways. *J. Clin. Invest.* **119,** 2925–2941
45. Vacher, P., Khadra, N., Vacher, A. M., Charles, E., Bresson-Bepoldin, L., and Legembre, P. (2011) Does calcium contribute to the CD95 signaling pathway? *Anti-cancer Drugs* **22,** 481–487
46. Rovere, P., Clementi, E., Ferrarini, M., Heltai, S., Sciorati, C., Sabbadini, M. G., Rugarli, C., and Manfredi, A. A. (1996) CD95 engagement releases calcium from intracellular stores of long term activated, apoptosis-prone gammadelta T cells. *J. Immunol.* **156,** 4631–4637
47. Wang, B., Nguyen, M., Breckenridge, D. G., Stojanovic, M., Clemons, P. A., Kuppig, S., and Shore, G. C. (2003) Uncleaved BAP31 in association with A4 protein at the endoplasmic reticulum is an inhibitor of Fas-initiated release of cytochrome *c* from mitochondria. *J. Biol. Chem.* **278,** 14461–14468
48. Martinou, J. C., and Youle, R. J. (2011) Mitochondria in apoptosis: Bcl-2 family members and mitochondrial dynamics. *Dev. Cell* **21,** 92–101
49. Breckenridge, D. G., Germain, M., Mathai, J. P., Nguyen, M., and Shore, G. C. (2003) Regulation of apoptosis by endoplasmic reticulum pathways. *Oncogene* **22,** 8608–8618